



## Thermodynamic and Adsorption Studies on the Corrosion Inhibition of Zn

### by 2, 2'-Dithiobis(2,3-dihydro-1,3-benzothiazole) in HCl Solutions

S. Abd El Wanees<sup>a,b,\*</sup>, Abeer Abdulaziz H. Bukhari<sup>c</sup>, Naifa S. Alatawi<sup>d</sup>, S.A. Khalil<sup>e</sup>, S. Nooh<sup>f</sup>, Syed Khalid Mustafa<sup>c</sup>, S. S. Elyan<sup>g</sup>



<sup>a</sup> University College of Umluj, University of Tabuk, Umluj, Tabuk, Saudi Arabia

<sup>b</sup> Chemistry Department, Faculty of Science, Zagazig University, Zagazig 44519, Egypt

<sup>c</sup> Department of Chemistry, Faculty of Science, University of Tabuk, Tabuk 71421, Saudi Arabia

<sup>d</sup> Physics Department, Faculty of Science, University of Tabuk, Tabuk 71421, KSA

<sup>e</sup> Chemistry Department, Alwajh-College, University of Tabuk, Tabuk, Saudi Arabia

<sup>f</sup> University College of Umluj, Computer Science Department, Umluj, Tabuk University, Saudi Arabia.

<sup>g</sup> Chemistry Department, Faculty of Pharmacy, Badr University, Badr, Egypt

### Abstract

The thermodynamics parameters and adsorption mechanism of 2,2'-dithiobis(2,3-dihydro-1,3-benzothiazole), DDBT, as a corrosion inhibitor for zinc in 0.5 M HCl solution were studied by different techniques. The used organic compound was prepared in our lab by a transformation reaction for thiol compound in the presence of ammonium per-sulfate. Potentiodynamic polarization, thermometric and gravimetric techniques, as well as, scanning electron microscope, SEM surface investigations were employed. The data of different techniques were compatible and confirmed the inhibition effect of DDBT. The potentiodynamic polarization data disclosed that the DDBT molecules behave as a mixed-kind inhibitor. The different thermodynamic parameters about the corrosion and adsorption processes such as  $E_a$ ,  $\Delta H_a$ ,  $\Delta S_a$ ,  $\Delta G^{\circ}_{ads}$ ,  $\Delta H^{\circ}_{ads}$  and  $\Delta S^{\circ}_{ads}$  were deduced to suggest the inhibition mechanism. The DDBT molecules are adsorbed on the Zn surface confirming the Langmuir isotherm model obeying a mixed mechanism (physical and chemisorption).

**Keywords:** Transformation Synthesis, 2,2'-Dithiobis(2,3-dihydro-1,3-benzothiazole), Adsorption; Zinc; Corrosion inhibitor; Thermodynamic; Langmuir isotherm.

### 1. Introduction

The general use of Zinc is the steel galvanization for protection from corrosion processes and as anode for chloride and alkaline batteries. The economic benefits come from its high capacity (0.82Ah/g), rechargeable batteries, and high discharge efficiency [1-3]. Great efforts have been done by many scientists to use some active minerals such as zinc for producing hydrogen gas when the metal becomes in contact with acids [4-10]. The produced  $H_2$ , which accompanies the corrosion reactions as an individual cathodic reaction in the aqueous acidic solution was found to depend on many parameters such as inundation time, the strength of the acid, and the solution temperature. The produced  $H_2$  gas delayed

by the presence of the corrosion products formed on the metal surface or the corrosion inhibitors that reduce the contact surface area to the aggressive media [11].

The employing of organic corrosion inhibitors is considered a significant controller to reduce the deteriorative effect of acidic media. Generally, compounds that contain O, S, P, and N are considered as effective corrosion inhibitors [12-14]. Recent literature about such compounds confirms the importance of the inhibition against the corrosion of zinc in hydrochloric acid aqueous solutions [15-20]. Such molecules can form a film through the active sites on the metal surface via the formation of an adsorbed protective layer protecting the metal from the corrosive effect of the medium.

\*Corresponding author e-mail: [s\\_nasr@ut.edu.sa](mailto:s_nasr@ut.edu.sa) & [s\\_wanees@yahoo.com](mailto:s_wanees@yahoo.com); (S.Abd El Wanees).

Receive Date: 07 September 2020, Revise Date: 20 September 2020, Accept Date: 27 September 2020

DOI: 10.21608/EJCHEM.2020.42128.2849

©2021 National Information and Documentation Center (NIDOC)

Benzothiazole derivatives could be considered as one of the most important types of organic inhibitors. This is due to the presence of electronegative such as N and S atoms besides the  $\pi$ -electrons of aromatic rings, which is easy to adsorb on the metal to form a protective film. The mechanism of inhibition of such compounds was found to depend on the adsorption process on the metal surface as well as the inhibitor concentration and temperature. The efficient adsorption could have resulted from the presence of the  $\pi$ -electrons inside the selected molecule beside the unsaturated bonds formed in the presence of the heteroatoms (S or O or N) in the inhibitor's molecular composition [21].

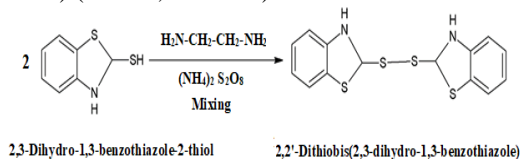
This study aimed to synthesize and evaluate the inhibition performance of dithiobis(2,3-dihydro-1,3-benzothiazole), DDBT, as an efficient retarder against the destruction of Zn in a 0.5 M HCl solutions. The material of DDBT is easily prepared in our laboratory with a high yield. The DDBT is easily soluble in dilute HCl and used as a corrosion inhibitor towards the  $H_2$  gas production when Zn reacted with HCl solution. Chemical (gravimetric and thermometric) and electrochemical (Tafel) techniques, complemented by surface investigations using the SEM technique were used.

## 2-Experimental

### 2.1. Materials and electrolyte

#### 2.1.1. Synthesis of DDBT inhibitor

The required inhibitor was prepared directly in the laboratory by a transformation reaction of thiol compound into disulfide by using ammonium persulfate in the presence of ethylenediamine [22]. The required amount of 2,3-dihydro-1,3-benzothiazole-2-thiol was weighed accurately in a mole unit (0.01 mole) and mixed thoroughly with the required amount of ethylenediamine (0.005 mole). The ammonium per-sulfate (0.011 mole) was added with continuous mixing using pestle and mortar for a while 40 min. After the accomplishment of the reaction, the crude product was extracted by using a dichloromethane solvent. The removal of the solvent under reduced pressure and the yield was recrystallized using ethanol. The synthetic route for the synthesis of 2,2'-dithiobis(2,3-dihydro-1,3-benzothiazole) (DDBT, inhibitor) is shown in scheme 1.



Scheme I. Synthetic route of 2,2'-dithiobis(2,3-dihydro-1,3-benzothiazole), DDBT.

#### 2.1.2. Material

Zn sheet (Johnson- Matthey, UK) was prepared in suitable samples with dimensions 0.3 cm x 5cm x 2 cm for the gravimetric and thermometric measurements. For the polarization experiments, a zinc rod (working electrode) has the same chemical composition were entrenched in epoxy resin leaving an exposed surface area of 0.28 cm<sup>2</sup>. The Zn sample was successively abraded with different grades of emery papers up to mirror finish. Then, it was washed with bi-distilled water, followed by rinsing with acetone, washed repeatedly with bi-distilled water, and finally immersed in the test solution. A fresh 0.5 M HCl solution was prepared using pure grade 37% HCl (BDH) and bi-distilled water. The inhibitor concentrations varied between  $1.0 \times 10^{-6}$  and  $1 \times 10^{-3}$  M freshly prepared in 0.5 M HCl before running the experiment. The substances of ethylenediamine, 2,3-dihydro-1,3-benzothiazole-2-thiol, and ammonium per-sulfate were obtained from Sigma-Aldrich Co., and Fluka Co., Germany chemicals.

#### 2.2. Experimental techniques

The potentiodynamic polarization was carried on Volta lab 80 (PGZ 402) potentiostat with Volta master 4 software under static conditions. Three electrodes system with Zn rode as a working electrode, a saturated calomel electrode, SCE, as a reference electrode and Pt wire as a counter electrode. The potential/current curves were obtained by sweeping the electrode potential at 2 mVs<sup>-1</sup> from  $E_{\text{initial}} = -1220$  mV to  $E_{\text{final}} = -800$  mV.

The reaction vessel and the procedure of thermometric experiments for following the dissolution temperature of Zn in HCl have been described previously [12, 23-25]. The used thermometric vessel was made of Pyrex glass (Mylius tube) kept inside a Dewar flask to minimize heat exchange with the surrounding. The starting solution temperature in all experiments was kept at 26 °C and the rise in the temperature was pursued with time to  $\pm 0.05$  °C, using a calibrated thermometer (0–100 °C). The reaction number,  $R_N$ , can be deduced from the relation [12, 23-25]:

$$R_N = \left( \frac{T_m - T_i}{t} \right), \text{ } ^\circ\text{C min}^{-1} \quad (1)$$

where  $T_i$  and  $T_m$  are initial and maximum temperatures, respectively, while,  $t$  is the immersion time attained when the temperature reaches  $T_m$ .

The gravimetric method was similar to that reported earlier [12, 23-25]. The mass of a clean polished Zn sample was determined before ( $m_1$ ) and after ( $m_2$ ) immersion in the test solution, for the desired time. The weight of each sample was determined using an analytical balance (precision  $\pm 0.001$ g). Each run was duplicated and the average mass loss was determined from the difference between  $m_2$  and  $m_1$  ( $\Delta m = m_1 - m_2$ ). The rate of the reaction,  $r_{\text{corr}}$ , expressed in  $\text{mg cm}^{-2} \text{min}^{-1}$  was calculated by using the following equation:

$$r_{\text{corr}} = \frac{\Delta m}{At} \quad (2)$$

where  $A$  is the total surface area of the Zn sample, and  $t$  is the immersion time. The surface coverage,  $\theta$ , and the inhibition efficiency,  $\eta_w$  %, were calculated, respectively, from  $r_{\text{corr}}$  values using the following equations:

$$\theta = \left(1 - \frac{r_{\text{corr}}}{r_{\text{corr}}^0}\right) \quad (3)$$

$$\eta_w = 100 (\theta) \quad (4)$$

where  $r_{\text{corr}}^0$  and  $r_{\text{corr}}$  are the rates of corrosion reaction in 0.5 M HCl in the absence and presence of the DDBT inhibitor, respectively.

### 2.3. Surface characterization analysis

The zinc specimens of size  $1 \text{ cm} \times 1 \text{ cm}$  were prepared as described above. The scanning electron microscope is used to investigate the surface morphology of some of the corroded Zn samples. The investigated samples were used before and after immersion for three hours in 0.5 M HCl without and with  $1 \times 10^{-4}$  M DDBT inhibitor. The working instrument was A Jeol type, JSM-5410 (Japan), has an accelerated voltage of 25 kV with a working distance of 20 mm.

## 3. Results and discussion

### 3.1. Polarization study.

The anodic and cathodic potentiodynamic polarization curves of Zn in 0.5 M HCl without and with various additions of DDBT are plotted in Fig. 1,

at 25 °C. It is cleared that, the cathodic and anodic curves are shifted to less active direction by the presence of different additives of DDBT due to the increase in the overvoltage accompanying the cathodic and anodic processes. Such behavior could prove that the mechanism of Zn dissolution and  $\text{H}_2$  evolution is under an activation-controlled process, and not altered by the presence of DDBT inhibitor [26, 27].

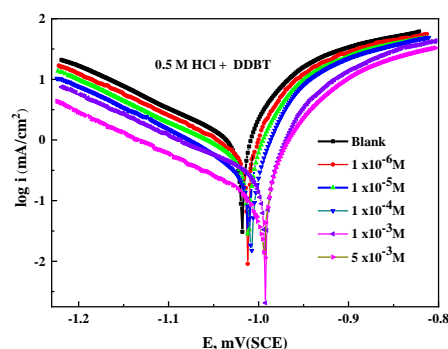


Fig 1. The potentiodynamic polarization curves of for Zn in 0.5 M HCl solution devoid of and containing different additions of DDBT inhibitor.

The surface coverage,  $\theta$ , and the inhibition efficiency  $\eta_p$  %, are determined using the following relations [26-30].

$$\theta = \left(\frac{I_{\text{corr}}^0 - I_{\text{corr}}}{I_{\text{corr}}^0}\right) \quad (5)$$

$$\eta_p = \left(\frac{I_{\text{corr}}^0 - I_{\text{corr}}}{I_{\text{corr}}^0}\right) 100 \quad (6)$$

where,  $I_{\text{corr}}^0$  and  $I_{\text{corr}}$  are the uninhibited and inhibited corrosion current densities of Zn in 0.5 M HCl, respectively. Table 1 displayed the electrochemical corrosion parameters, viz., corrosion potential ( $E_{\text{corr}}$ ), corrosion current density ( $I_{\text{corr}}$ ), anodic ( $\beta_a$ ), cathodic ( $\beta_c$ ) Tafel slopes, surface coverage,  $\theta$ , the percentage of inhibition efficiency ( $\eta_p$  %) and the standard deviation,  $\sigma$ . Inspection of the data of Table 1 reveals that, both the values of  $\theta$  and  $\eta_p$  % increase with increasing the inhibitor concentration. The increase in the DDBT concentration is accompanied by the reduction in the corrosion current density ( $I_{\text{corr}}$ ) with a corresponding increase in the values of  $\theta$  and  $\eta_p$  %.

**Table 1:** The polarization parameters ( $E_{\text{corr}}$ ,  $\beta_a$ ,  $\beta_c$ ,  $I_{\text{corr}}$ ,  $\theta$  and  $\eta_p$  %) and the standard deviation,  $\sigma$ , corresponding the inhibition efficacy, for Zn corrosion in 0.5 M HCl containing different concentrations of DDBT inhibitor, at 25°C.

Conc., M	$-E_{\text{corr}}$ , mV	$\beta_a$ , mV/dec	$-\beta_c$ , mV/dec	$I_{\text{corr}}$ , mAcm <sup>-2</sup>	$\theta$	$\eta_p$ %	Standard deviation, $\sigma$ ,
Free acid	1017	42	131	0.79	--	--	
1 x 10 <sup>-6</sup>	1013	43	141	0.45	0.423	42.31	8.8
1x 10 <sup>-5</sup>	1011	39	136	0.34	0.564	56.41	3.5
1 x 10 <sup>-4</sup>	1007	38	130	0.29	0.628	62.82	8.4
5 x 10 <sup>-4</sup>	993	35	165	0.21	0.731	73.08	6.4
1 x 10 <sup>-3</sup>	990	37	167	0.15	0.821	82.05	6.6

**Table 2:** The values of the reaction number,  $R_N$ , surface coverage,  $\theta$ , and the inhibition efficiency,  $\eta_R$  %, for the corrosion of Zn in 0.5 M HCl in the presence of different concentrations of DDBT inhibitor.

Concentration	$R_N$ , °C.min <sup>-1</sup>	$\theta$	$\eta_R$ %
Free acid	1.948	--	
1 x 10 <sup>-6</sup> M	1.469	0.246	24.6
5 x 10 <sup>-6</sup> M	1.110	0.430	43.5
1 x 10 <sup>-5</sup> M	0.745	0.618	61.8
1 x 10 <sup>-4</sup> M	0.397	0.796	79.6
5 x 10 <sup>-4</sup> M	0.196	0.899	89.9
1 x 10 <sup>-3</sup> M	0.103	0.947	94.7

The values of  $\eta_p$  % for the different concentrations of the DDBT inhibitor, obtained by the three different experimental techniques, potentiodynamic polarization, thermometric and gravimetric techniques are collected in Tables 1 and 2. The standard deviation values,  $\sigma$ , of the inhibitory efficiencies calculated by the three techniques are included in Table 1. The  $\sigma$  values were varied between 3.5 and 8.8, depending on the inhibitor concentration, which confirms the good agreement between the used techniques. The relatively high values of  $\sigma$  could be attributed to the difference in the acid concentration with the thermometric method (1.0 M HCl) than other methods (0.5 M HCl) besides the experimental conditions of each technique.

Also, the non-significant changes in the values of  $\beta_a$  and  $\beta_c$ , besides the little displacement in  $E_{\text{corr}}$  (4-27 mVSCE), which less than 85 mV, confirm that the used inhibitor is considered as a mixed-type inhibitor [31-36].

### 3.2. Thermometric study

The effect of the addition of DDBT inhibitor on the corrosion of zinc in 1.0 M HCl solution was

investigated by the thermometric technique. Fig 2 depicts the temperature-time relations for Zn in 1.0 M HCl solution devoid of and containing different additions of DDBT inhibitor. The presence of DDBT inhibitor decreases the reaction number,  $R_N$  (Table 2) through a decrease in  $T_m$  and an elongation of the time,  $t$  needed to attain  $T_m$ . This behavior is due to the retardation in the corrosion reaction, the  $R_N$  values are used to express the rate of reaction in the free acid and inhibitive solutions.

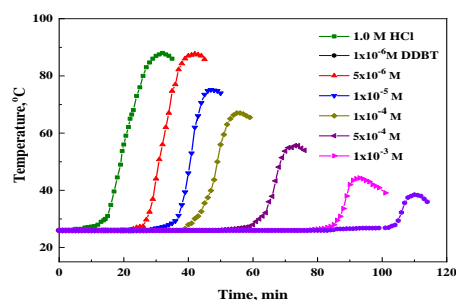


Fig 2. Variation of the temperature with the immersion time for Zn in 1.0 M HCl solution devoid of and containing different additions of DDBT.

**Table 3:** Different gravimetric data for the corrosion of Zn in 0.5 M HCl in the absence and presence of different concentrations of DDBT inhibitor, at different temperatures.

T, k	Parameter	Free acid	1x10 <sup>-6</sup> M	1x10 <sup>-5</sup> M	1x10 <sup>-4</sup> M	1x10 <sup>-3</sup> M
298	$r_{\text{corr}}$ , $\mu\text{g cm}^{-2}\cdot\text{min}^{-1}$	2.543	1.655	1.142	0.478	0.210
	$\theta$	--	0.349	0.551	0.808	0.917
	$\eta_{\text{w}}$ %	--	34.90	55.10	80.80	91.70
303	$r_{\text{corr}}$ , $\mu\text{g cm}^{-2}\cdot\text{min}^{-1}$	2.745	1.921	1.395	0.825	0.345
	$\theta$	--	0.300	0.492	0.768	0.873
	$\eta_{\text{w}}$ %	--	30.00	49.20	76.80	87.30
308	$r_{\text{corr}}$ , $\mu\text{g cm}^{-2}\cdot\text{min}^{-1}$	2.957	2.215	1.712	0.869	0.470
	$\theta$	--	0.251	0.421	0.706	0.841
	$\eta_{\text{w}}$ %	--	25.10	42.10	70.60	84.10
313	$r_{\text{corr}}$ , $\mu\text{g cm}^{-2}\cdot\text{min}^{-1}$	3.177	2.571	2.083	1.083	0.799
	$\theta$	--	0.191	0.344	0.659	0.749
	$\eta_{\text{w}}$ %	--	19.10	34.40	65.90	74.85
318	$r_{\text{corr}}$ , $\mu\text{g cm}^{-2}\cdot\text{min}^{-1}$	3.385	2.942	2.356	1.441	0.951
	$\theta$	--	0.131	0.304	0.574	0.719
	$\eta_{\text{w}}$ %	--	13.10	30.40	57.40	71.91

A plot of the reaction number,  $R_N$ , as a function of the logarithm of the molar concentration of the added DDBT inhibitor, gives a sigmoidal S-shaped curve, Fig 3, which confirms the presence of an adsorption step [12, 24]. It is cleared that increasing the DDBT inhibitor concentration reduces the  $R_N$  values, lowering the corrosion rate due to the adsorption of the inhibitor molecules on the Zn surface producing a protective film.

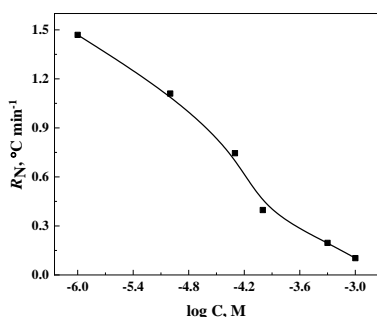


Fig 3. Variation of the reaction number,  $R_N$ , as a function of the logarithm of the molar concentration of the added DDBT inhibitor.

The  $R_N$  values at different additions of DDBT inhibitor are used to calculate the surface coverage,  $\theta$ , and the inhibition efficiency,  $\eta_N$ , according to the following equation [12, 24, 25]:

$$\theta = \left(1 - \frac{R_N}{R_N^0}\right) \quad (7)$$

$$\eta_N = \left(1 - \frac{R_N}{R_N^0}\right) 100 \quad (8)$$

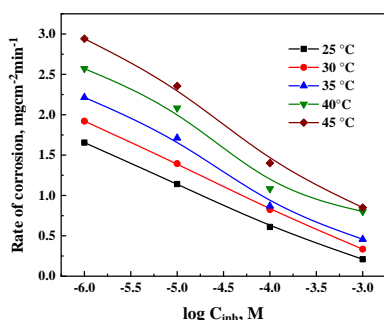
where  $R_N^0$  and  $R_N$  are the reaction numbers in the absence and presence of the DDBT inhibitor, respectively. The values of  $\theta$  and  $\eta_N$ , of the DDBT inhibitor, are listed in Table 2. The data reveals that the values of  $\theta$  and  $\eta_N$  are increased as the inhibitor concentration is increased confirming the inhibition of Zn corrosion in 1.0 M HCl, which is consistent with the data obtained by other used techniques.

### 3.3. Gravimetric study

The gravimetric study is used to confirm the inhibition effect on the corrosion of Zn in 0.5 M HCl when different additions of DDBT inhibitor, at various temperatures. The data are used to determine the different corrosion parameters such as corrosion rate,  $r_{\text{corr}}$  (mg/cm<sup>2</sup>/h),  $\theta$  and  $\eta_w$ , Table 3. Fig 4 depicts the variation in the corrosion reaction rate,  $r_{\text{corr}}$ , with the logarithm of the molar concentration of the added DDBT inhibitor. It is clear that the rate of reaction,  $r_{\text{corr}}$ , raises with the temperature in the case of the free and the inhibited solutions, although it decreases as the inhibitor concentration is raised, at a fixed temperature. The higher additions of DDBT inhibitor cause more lowering in the corrosion rate and gives high values for the surface coverage,  $\theta$ , and the inhibition efficacy,  $\eta_w$ , Table 3. The sigmoid nature of  $\eta_w - \log C_{\text{inh}}$  curves, of Fig 4 could confirm the adsorptive ability of the DDBT inhibitor towards the Zn metal surface [12]. The decrease in the inhibition efficiency values,  $\eta_w$ , for the DDBT inhibitor at high temperature (Fig 4) could be related to the desorption of some of the DDBT molecules with the rise in the temperature [37].

**Table 4:** Adsorption parameters for DDBT inhibitor on the Zn surface in 0.5 M HCl, obtained from Langmuir adsorption isotherm at different temperatures

T, K	R <sup>2</sup>	K <sub>ads</sub> ,	ΔG <sup>o</sup> <sub>ads</sub> ,	ΔH <sup>o</sup> <sub>ads</sub> ,	ΔS <sup>o</sup> <sub>ads</sub> ,
		M <sup>-1</sup>	kJ/mol	kJ mol <sup>-1</sup>	J mol <sup>-1</sup> K <sup>-1</sup>
298	0.9998	11.03x10 <sup>4</sup>	38.72		332
303	0.9997	7.11x10 <sup>4</sup>	38.26		325
308	0.9999	3.85x10 <sup>4</sup>	38.12	60.19	319
313	0.9997	3.27x10 <sup>4</sup>	37.50		312
318	0.9988	2.43x10 <sup>4</sup>	37.31		307

Fig 4. Variation of the corrosion reaction rate,  $r_{\text{corr}}$ , as a function of the logarithm of the molar concentration of the added DDBT inhibitor.

Furthermore, comparison and validation of the obtained results, inhibition efficiency, is an important phase of search studies. Besides, the variation of inhibition efficiency  $\eta$  (%) gained by the three experimental techniques used in this study, as a function of DDBT concentration in 0.5 M HCl is presented in Tables 1-3.

### 3.4. Adsorption behaviour

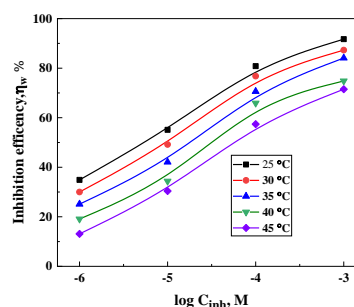
The adsorption of the organic inhibitors on the investigated metal surface in aggressive aqueous solutions can be attributed to the presence of lone pair of electrons on the heteroatoms of the inhibitor molecules. Adsorption of inhibitor is considered a substitution process in which an exchange between adsorbed H<sub>2</sub>O molecules and organic molecules takes place.

The surface coverage,  $\theta$ , calculated from the data of gravimetric measurements is used as a function of the used inhibitor concentration, to scrutinize the type of adsorption isotherm. The isotherm accounts for the

nature of the interaction between the inhibitor molecules and the metal. In this investigation, the best-fit isotherm was the Langmuir model. The applicable isotherm can be achieved from the relation [38, 39]:

$$\frac{C_{\text{inh}}}{\theta} = \frac{1}{K_{\text{ads}}} + C_{\text{inh}} \quad (9)$$

The plotting of  $C_{\text{inh}}/\theta$  vs  $C_{\text{inh}}$ , at different temperatures, give straight lines, as shown in Fig 6. The values of the slope and  $r$  are approximately equal to one, which confirms the adsorption of DDBT on the Zn surface according to the Langmuir's isotherm. The corresponding linear regression coefficient ( $r^2$ ), and the adsorption equilibrium constant,  $K_{\text{ads}}$  are collected in Table 4. High values of  $K_{\text{ads}}$  for studied inhibitor reflect strong interaction of DDBT with Zn surface [40] confirming strong adsorption of DDBT on the metal surface in 0.5 M HCl. The depress in  $K_{\text{ads}}$  values with temperature (Table 4) indicates a drop in the adsorptive ability due to the desorption of DDBT molecules on the Zn surface [41].

Fig 5. Variation of the inhibition efficiency,  $\eta_w$ , as a function of the logarithm of the molar concentration of the added DDBT inhibitor.



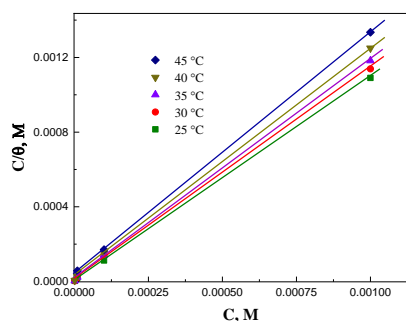


Fig 6. Langmuir adsorption isotherm for DDBT inhibitor on the Zn surface in 0.5 M HCl at different temperatures.

### 3.5. Adsorption thermodynamic parameters

The equilibrium constant for the adsorption process,  $K_{ads}$  is used to calculate the standard free energy of adsorption,  $\Delta G^{\circ}_{ads}$ , using the equation [42]:

$$K_{ads} = \frac{1}{55.5} \exp\left(\frac{-\Delta G^{\circ}_{ads}}{RT}\right) \quad (10)$$

where 55.5 is the molar concentration value of  $H_2O$  in mol/L and R is the universal gas constant. The calculated values of  $\Delta G^{\circ}_{ads}$  are recorded in Table 4. The negative sign of  $\Delta G^{\circ}_{ads}$  secures the spontaneity of the adsorption process and fastness of the adsorbed DDBT film on the Zn surface. When  $\Delta G^{\circ}_{ads}$  values around  $-40 \text{ kJ mol}^{-1}$  or more negative allude to the chemisorption type, while those around  $-20 \text{ kJ mol}^{-1}$  or less negative are correlating to physical adsorption [43, 44]. In our case, the calculated values of  $\Delta G^{\circ}_{ads}$  (Table 6) were  $-38.72$ ,  $38.26$ ,  $-38.12$ ,  $-37.50$  and  $-37.31 \text{ kJ mol}^{-1}$  at 25, 30, 35, 40, 45°C, respectively. These values confirm that a mixed chemi and

**Table 5:** Activation parameters of dissolution reaction of Zn in 0.5 M HCl containing different concentrations of DDBT inhibitor.

Conc, M	$E_a$ , $\text{kJ mol}^{-1}$	$\Delta H_a$ , $\text{kJ mol}^{-1}$	$-\Delta S_a$ , $\text{J mol}^{-1}$
Free	11.35	10.5	208
$1 \times 10^{-6} \text{ M}$	22.73	20.2	173
$1 \times 10^{-5} \text{ M}$	31.02	28.4	149
$1 \times 10^{-4} \text{ M}$	32.33	34.9	133
$1 \times 10^{-3} \text{ M}$	68.98	66.4	035

physisorption is involved in the inhibition process [45, 46].

Adsorption thermodynamic parameters are employed to elucidate the adsorption behaviour of DDBT on the Zn surface. The standard enthalpy of adsorption ( $\Delta H^{\circ}_{ads}$ ) can be calculated from the Van't Hoff equation [40].

$$\frac{d \ln K_{ads}}{dT} = \frac{\Delta H^{\circ}_{ads}}{RT^2} \quad (11)$$

where R is the gas constant ( $8.314 \text{ J K}^{-1} \text{ mol}^{-1}$ ) and T is the absolute temperature (K). The indefinite integration of equation 11 can give [45]:

$$\ln K_{ads} = -\left(\frac{\Delta H^{\circ}_{ads}}{RT}\right) + \text{constant} \quad (12)$$

The values of  $\ln K_{ads}$  are plotted against  $1/T$ , Fig 7, to give a straight-line relation, with a slope equal to  $-\Delta H^{\circ}_{ads}/R$ . The value of  $\Delta H^{\circ}_{ads}$  is found to be  $-60.19 \text{ kJ/mol}$ , Table 4. It has been reported that the endothermic adsorption process ( $\Delta H^{\circ}_{ads} > 0$ ) is accompanied to chemisorption process, while the exothermic adsorption process ( $\Delta H^{\circ}_{ads} < 0$ ) may be attributed to physisorption, chemisorption, or a mixture of both adsorption processes [46]. The negative sign of the obtained  $\Delta H^{\circ}_{ads}$  indicates the exothermic nature of adsorption of DDBT on the Zn surface in 0.5 M HCl. From the other side, the value of enthalpy is  $< 100 \text{ kJ mol}^{-1}$ , which announces that the adsorption of DDBT on Zn surface is not merely physical or chemical, but the mixed type [38, 40]. For the chemisorption process,  $\Delta H^{\circ}_{ads}$  approaches  $100 \text{ kJ mol}^{-1}$ , while for the physisorption process, it is less than  $40 \text{ kJ mol}^{-1}$  [47].

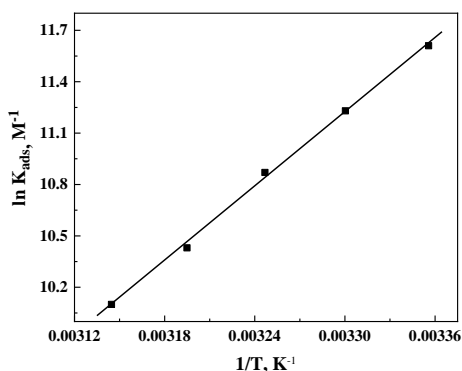


Fig 7. Van't Hoff plot for zinc in 0.5 M HCl with DDBT inhibitor.

The standard adsorption of entropy,  $\Delta S_{ads}^{\circ}$ , can also obtain from the following equation [46, 48]:

$$\Delta S_{ads}^{\circ} = \frac{\Delta H_{ads}^{\circ} - \Delta G_{ads}^{\circ}}{T} \quad (13)$$

The values of  $\Delta S_{ads}^{\circ}$  can be calculated and collected in Table 4. The positive values of  $\Delta S_{ads}^{\circ}$  suggest that adsorption is accompanied by an increase in the disorder system due to the adsorption of inhibitor molecules on the Zn surface [49].

### 3.6. Effect of temperature

The effect of temperature on the corrosion of Zn was further examined at different temperatures (298 – 338 K) to explore and deduce the activation corrosion parameters in the 0.5 M HCl in the absence and presence of different concentrations of DDBT inhibitor. The values of  $r_{corr}$  are found to increase with the raise the temperature, in the case of the free acid and the inhibitive solutions. Temperature enhances the rate of diffusion of  $H^+$  ions to the metal surface, as well as the ionic mobility [12, 43]. The decrease in  $r_{corr}$  values, in the case of inhibitor, confirms the decrease in each of the anodic metal dissolution and the corresponding cathodic  $H_2$  production, without altering the mechanism of the reaction.

The required apparent activation energy,  $E_a$ , can be calculated using Arrhenius equation [38, 50]:

$$r_{corr} = A \exp\left(\frac{-E_a}{RT}\right) \quad (14)$$

where  $r_{corr}$  is the rate of corrosion reaction calculated by the gravimetric method, A represents the Arrhenius factor, T is the absolute temperature and R = 8.314J mol<sup>-1</sup> is the universal gas constant.

However, the values of  $E_a$  can be determined mathematically from the Arrhenius graph, Fig 8 (variation of  $\log r_{corr}$  against  $T^{-1}$ ), and are given in Table 5. The obtained value of  $E_a$  for Zn in the blank solution is 11.35 kJ/mol. In the presence of different concentrations of DDBT,  $E_a$  varied between 22.73 and 68.98 kJ/mol depending on the inhibitor concentration. The increase in activation energy  $E_a$  in presence of DDBT indicates that the retardation in the corrosion rate is controlled by the adsorption of the inhibitor on the Zn surface [51, 52]. Moreover, the increase in  $E_a$  with the inhibitor is often supporting the physical adsorption mechanism [53].

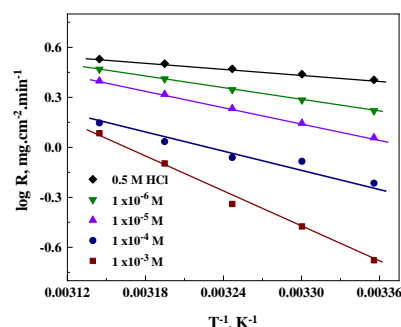


Fig 8. Arrhenius plots for the corrosion rate of Zn in 0.5 M HCl in absence and in presence of different concentrations of DDBT.

The values of  $r_{corr}$  ( $mgcm^{-2}min^{-1}$ ) at different temperatures are used to locate the values of apparent enthalpy of activation  $\Delta H_a$  and apparent entropy of activation  $\Delta S_a$  for the formation of the activation complex, using transition state equation [37, 50–52]:

$$r_{corr} = \frac{RT}{Nh} \exp\left(\frac{\Delta S_a}{R}\right) \exp\left(\frac{-\Delta H_a}{RT}\right) \quad (15)$$

where h is Planck's constant and N is the Avogadro's number. From the linear plot of  $\log(r_{corr}/T)$  vs  $T^{-1}$ , Fig 9,  $\Delta H_a$  and  $\Delta S_a$  were calculated using the slope



and the intercept, successively, obtained by the linear fit, Table 5. The positive sign of  $\Delta H_a$  reflects the endothermic nature of Zn dissolution in the absence and presence of inhibitor. The increase in the values of  $\Delta H_a$  in presence of DDBT means that the dissolution of Zn becomes more difficult in the presence of the inhibitor [53]. The negative value of  $\Delta S_a$  (Table 4) indicates that the activated complex in the rate-determining step represents an association rather than a dissociation step, meaning that a decrease in disorder takes place during the transition from reactant to the activated complex [54]

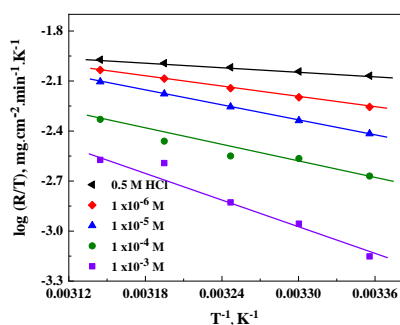


Fig 9. Transition-state plots for the corrosion rate of Zn in 0.5 M HCl in absence and in presence of different concentrations of DDBT.

### 3.7. Surface morphology.

The surface investigation has been carried out to Zn surfaces to understand the surface properties and morphology during the electrochemical corrosion behaviour. Figs 10 (A, B) show the SEM micrographs after immersion for 3 hr in 0.5 M HCl solution (A) without inhibitor and (B) with  $1 \times 10^{-5}$  M DDBT, at 25 °C. The SEM micrograph of the corroded Zn sample in 0.5 M HCl solution (10A) shows a uniform damaged Zn surface covered by corrosion products. The large corroded areas might probably have been formed from smaller pits expanded equally laterally, as well as, inwardly so that it takes the shape of large attacked areas. In contrast, in the presence of the inhibitor, less damage surface with little numbers of pits can be seen on the zinc surface (10B). Therefore, the presence of the inhibitor decreased the rate of corrosion Zn in 0.5 M HCl.

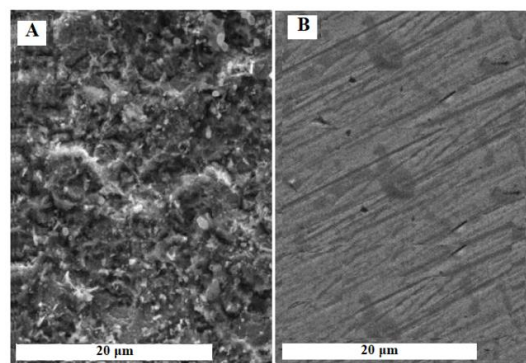


Fig 10. The SEM micrographs for Zn surface after immersion for 3hr in (A) 0.5 M HCl and (B) 0.5 M HCl containing  $1 \times 10^{-4}$  M DDBT inhibitor, at 25 °C.

### 3.8. Inhibition mechanism

The corrosion protection of Zn by 2,2'-dithiobis(2,3-dihydro-1,3-benzothiazole), DDBT is attributed to the adsorption through the active sites on the metallic surface (Zn/HCl interface) to form a protective film. The adsorption of this inhibitor is facilitated by the presence of heteroatoms of N and S on the inhibitor molecule with lone pairs of free electrons beside the electrons of two benzene rings already included in the molecule. The formed film isolates the metal surface from the aggressive medium preventing direct contact with the aggressive acid. The adsorption of DDBT molecules at Zn/HCl water interface can be regarded as a replacement process between DDBT<sub>aq</sub> and water molecules on the Zn surface, H<sub>2</sub>O<sub>ads</sub>



where  $x$  is the number of water molecules replaced by a molecule of DDBT<sub>ads</sub>. DDBT<sub>ads</sub> molecules can adsorb on the Zn surface via the lone pair of free electrons located on the N and S atoms without ignoring the effective conjugated role of the  $\pi$ -electrons system in the molecule [8, 9].

From the second point of view, a protonated inhibitor species DDBTH<sup>+</sup><sub>ads</sub> is easily formed in the acidic medium. The formed DDBTH<sup>+</sup><sub>ads</sub> charged molecules electrostatically interact with ZnCl<sub>2</sub><sub>ads</sub>, so the oxidation of Zn to form ZnCl<sub>2</sub> can be prevented. Also, since the discharge of H<sup>+</sup> ions to form adsorbed H atoms on the Zn surface is the rate-determining

step, the adsorption of efficient  $\text{DDBT}_{\text{ads}}$  molecules will almost cover the surface leading to retardation of discharge of  $\text{H}^+$  ions [9].

At lower concentrations of the adsorbed inhibitor, the formed  $\text{Zn DDBTH}_{\text{ads}}$  is more soluble and its concentration is not enough to cover the Zn surface. Therefore, the corrosion process takes place on the sites free from  $\text{Zn DDBTH}_{\text{ads}}$ . When  $\text{DDBTH}_{\text{sol}}$  concentration is high enough, a compact and coherent inhibitor layer is formed on the Zn surface, reducing the corrosion process.

#### 4. Conclusions

1. The rate of  $\text{H}_2$  production increases with the immersion time and the solution temperature.
2. Small additions of 2,2'-dithiobis(2,3-dihydro-1,3-benzothiazole), DDBT decrease the corrosion rate as confirmed from the data of Tafel and EIS techniques.
3. Polarization data indicate that 2,2'-dithiobis(2,3-dihydro-1,3-benzothiazole), DDBT is a mixed inhibitor.
4. The inhibition efficiency is increased with increasing inhibitor concentration and a decrease with the temperature.
5. The adsorption process is mixed between physical and chemical processes according to Langmuir isotherm.
6. The adsorption process is mixed between physical and chemical processes according to Langmuir isotherm.

#### 5. Conflicts of interest

There are no conflicts to declare.

#### 6. Acknowledgment

The authors would like to extend their appreciation to

the Deanship of Scientific Research at the University of Tabuk for funding this work through research group number S-1441-0146.

#### References

1. O. Abootalebi, A. Kermanpur, M. R. Shishesaz, M. A. Golozar, Optimizing the electrode position in sacrificial anode cathodic protection systems using boundary element method, *Corros. Sci.*, 52 (2010) 678-687.
2. S. Manov, F. Noli, A. M. Lamazouere, L. Aries, Surface treatment for zinc corrosion protection by a new organic chelating reagent, *J. Appl. Electrochem.*, 29 (1999) 995-1003.
3. F. Wang, F. Yu, X. Wang, Z. Chang, L. Fu, Y. Zhu, Z. Wen, Y. Wu, W. Huang, Aqueous rechargeable zinc/aluminum ion battery with good cycling performance, *ACS Appl. Mater. Interfaces*, 14 (2016) 9022-9029.
4. S. Abd El Wanees, N. M. El Basiony, A.M. Al-Sabagh, M. A. Alsharif, M. A. Migahed, Controlling of  $\text{H}_2$  gas production during Zn dissolution in HCl solutions, *J. Mol. Liq.*, 248 (2017) 248 943-952.
5. M. Abdalla, Ethoxylated fatty acids as corrosion inhibitors for dissolution of zinc in hydrochloric acid, *Corros. Sci.*, 89 (2003) 2705-2716.
6. E. E. Foad El-Sherbini, S. M. Abd El Wahaab, M. A. Deyab, Ethoxylated fatty acids as inhibitors for the corrosion of zinc in acid media, *Mater. Chem. Phys.*, 89 (2005) 183-191
7. S. Abd El Wanees, M. I. Alahmdi, M. A. Alsharif, Y. Atef, Mitigation of hydrogen evolution during zinc corrosion in aqueous acidic media using 5-Amino-4-imidazolecarboxamide, *Egypt. J. Chem.*, 62 (2019) 811-825.
8. M. G. A. Saleh, S. Abd El Wanees, S. Khalid Mustafa, Dihydropyridine derivatives as controllers for production of hydrogen during zinc dissolution, *Chem. Eng. Commun.*, 206 (2019) 789-803
9. S. Abd El Wanees, S. H. Seda, Corrosion Inhibition of zinc in aqueous acidic media using a novel synthesized Schiff Base—an experimental and theoretical study, *J. Disper. Sci. Techn.*, 40 (2019) 1813-1826.

10. M. Abdallah, S. A. Ahmed, H. M. Altass, I. A. Zaafarany, M. Salem, A. I. Aly, E. M. Hussein. Competent inhibitor for the corrosion of zinc in hydrochloric acid based on 2,6-bis-[1-(2-phenylhydrazono)ethyl]pyridine, *Chem. Eng. Commun.*, 206 (2019) 137-148.
11. M. A. Deyab, Hydrogen generation during the corrosion of carbon steel in crotonic acid and using some organic surfactants to control hydrogen evolution, *Int. J. Hydrogen Energy*, 38 (2013) 13511-13519.
12. S. M. And El Haleem, S Abd El Wanees, E. E. Abd El Aal, A. Farouk, Factors affecting the corrosion behaviour of aluminium in acid solutions. I. Nitrogen and/or sulphur-containing organic compounds as corrosion inhibitors for Al in HCl solutions, *Corros. Sci.*, 68 (2013) 1-13.
13. S. Abd El Wanees, M. I. Alahmdi, M. Abd El Azzem, H. E. Ahmed, 5, 6-Dimethyl-2-oxo-1, 2-dihydropyridine-3-carboxylic acid as an inhibitor towards the corrosion of C-steel in acetic acid, *Inter. J. Electrochem. Sci.*, 11 (2016) 3448-3466.
14. S. Abd El Wanees, M. I. Alahmdi, S. M. Rashwan, M. M. Kamel, Inhibitive Effect of cetyltriphenyl- phosphonium bromide on C-steel corrosion in HCl solution, *Inter. J. Electrochem. Sci.*, 11 (2016) 9265-9281.
15. M. Abdallah, S. T. Atwa, M. M. Salem, A. S. Fouda, Synergistic effect of some halide Ions on the inhibition of zinc corrosion in hydrochloric acid by tetrahydrocarbazole derivatives compounds, *Int. J. Electrochem. Sci.*, 8 (2013) 10001 – 10021.
16. M. Abdalla, I. Zaafarany, A. S. Fouda, and D. Abd El-Kader, Inhibition of Zinc corrosion by some benzaldehyde derivatives in HCl solution, *J. Mater. Eng. and Performance*, 21 (2012) 995-1002.
17. M. Abdallaha, I. A. Zaafarany, B.A. AL Jahdaly, Corrosion inhibition of zinc in hydrochloric acid using some antibiotic drugs, *J. Mater. Environ. Sci.*, 7 (2016) 1107-1118.
18. M. Abdallah, , S. A. Ahmed, H.M. Altass, I.A. Zaafarany, M. Salem, A.I. Aly, E.M. Hussein, Competent inhibitor for the corrosion of zinc in hydrochloric acid based on 2,6-bis-[1-(2-phenylhydrazono)ethyl]pyridine, *Chem. Eng. Comm.*, 206 (2019)137-148.
19. A. M. Guruprasad, H. P. Sachin, G. A. Swetha, B. M. Prasanna, Corrosion inhibition of zinc in 0.1 M hydrochloric acid medium with clotrimazole: Experimental, theoretical and quantum studies, *Surfaces and Interfaces*, 19 (2020) 100478.
20. H. M. Abd El-Lateef, M. EL Roubay, Synergistic inhibition effect of poly(ethylene glycol) and cetyltrimethylammonium bromide on corrosion of Zn and Zn—Ni alloys for alkaline batteries, *Transactions of Nonferrous Metals Society of China*, 30 (2020) 259-274.
21. K. C. Emregul, O. Atakol, Corrosion inhibition of mild steel with Schiff base compounds in 1M HCl, *Mater. Chem. Phys.*, 82 (2003) 188-193
22. R.S. Verma, H.M. Meshram, R. Dahiya, Solid state oxidation of thiols to disulfides using ammonium per-sulfate, *Synth. Commun.*, 30 (2000) 1249-1255.
23. S. Abd El Wanees, E. E. Abd El Aal, A Abd El Aal, The inhibitive effect of some alcohols towards the corrosion of lead in nitric acid, *Bull. Soc. Chim. Fr*, 128 (1991) 889-893.
24. E. E. Abd El Aal, S. Abd El Wanees, A. Farouk, S.M. Abd El Haleem Factors affecting the corrosion behaviour of aluminium in acid solutions. II. Inorganic additives as corrosion inhibitors for Al in HCl solutions, *Corros. Sci.* 68(2013) 14-24.
25. S. Abd El Wanees. Amines as inhibitors for corrosion of copper in nitric acid, *Anti-Corros. Methods Mater.*, 41 (1994) 3–7.
26. M. A. Ameer, A. M. Fekry, Inhibition effect of newly synthesized heterocyclic organic molecules on corrosion of steel in alkaline medium containing chloride, *Int. J. hydrogen energy*, 35 (2010)11387-11396.
27. M. A. Amin, M. A. Ahmed, H. A. Arida, T. Arslan, M. Saracogiu, F. Kandemirli, Monitoring corrosion and corrosion control of iron in HCl by non-ionic surfactants of the TRITON-X series– Part II. Temperature effect, activation energies and thermodynamics of adsorption, *Corros. Sci.*, 53 (2011) 540-548.
28. S. Abd El Wanees, A. Diab, O. Azazy, M. Abd El Azim, Inhibition effect of N-(pyridin-2-yl-

- carbamothioyl)benzamide on the corrosion of C-steel in sulfuric acid solutions, *J. Disper Sci Technol.*, 35 (2014) 1571-1580.
29. S. Abd El Wanees, E. E. Abd El Aal, N-Phenylcinnamimide and some of its derivatives as inhibitors for corrosion of lead in HCl solutions, *corros. Sci.*, 52 (2010) 338-344.
30. SM Abd El Haleem, S Abd El Wanees, A Bahgat, Environmental factors affecting the corrosion behaviour of reinforcing steel. VI. Benzotriazole and its derivatives as corrosion inhibitors of steel *Corr. Sci.*, 87 (2014) 321-333.
31. T. Poornima, J. Nayak, A.N. Shetty, 3, 4 - Dimethoxy benzaldehyde thiosemicarbazone as corrosion inhibitor for aged 18Ni 250 grade maraging steel in 0.5 M sulfuric acid, *J. Appl. Electrochem.*, 41 (2011) 223 - 233.
32. W. H. Li, Q. He, S.T. Zhang, C.I. Pei, B. R. Hou, Some new triazole derivatives as inhibitors for mild steel corrosion in acidic medium, *J. Appl. Electrochem.*, 38 (2008) 289 – 295.
33. E.S. Ferreira, C. Giancomlli, F.C. Giacomlli, A. Spinelli, Evaluation of the inhibitor effect of L-ascorbic acid on the corrosion of mild steel, *Mater. Chem. Phys.*, 83 (2004) 129–134.
34. T. K. Chaitra, K. N. Shetty Mohana, H. C.Tandon, Thermodynamic, electrochemical and quantum chemical evaluation of some triazole Schiff bases as mild steel corrosion inhibitors in acid media, *J. Mol. Liq.*, 211 (2015) 1026–1038.
35. N. Labjar, M. Lebrini, F. Bentiss, N. Chihib, S. El Hajjaji, C. Jama, Corrosion inhibition of carbon steel and antibacterial properties of aminotris-(methylenephosphonic) acid, *Mat. Chem. Phys.*, 119 (2010) 330–336
36. H. Ashassi-Sorkhabi, N. Ghalebsaz-Jeddi, F. Hashemzadeh, H. Jahani, Corrosion inhibition of carbon steel in hydrochloric acid by some polyethylene glycols, *Electrochim. Acta*, 51(2006) 3848-3858.
37. A.K. Maayta, N.A.F. Al-Rawashdeh, Inhibition of acidic corrosion of pure aluminum by some organic compounds, *Corros. Sci.*, 46 (2004) 1129-1140.
38. S. Abd El Wanees, A. B. Radwan, M.A. Alsharif, S. M. Abd El Haleem, Initiation and inhibition of pitting corrosion on reinforcing steel under natural corrosion conditions, *Mater. Chem. Phys.*, 190 (2017)79-95.
39. M. G. Saleh, S. Abd El Wanees, S. K. Mustafa, Dihydropyridine derivatives as controllers for production of hydrogen during zinc dissolution, *Chem. Eng. Commun.*, 206 (2019) 789-803.
40. X.H. Li, S.D. Deng, H. Fu, G.N. Mu, Inhibition by tween-85 of the corrosion of cold rolled steel in 1.0 M hydrochloric acid solution, *J. Appl. Electrochem.*, 39 (2009) 1125–1135.
41. Li Feng, S. Zhang, Y. Lu, B. Tan, S. Chen, L. Guo, Synergistic corrosion inhibition effect of thiazolyl-based ionic liquids between anions and cations for copper in HCl solution, *Appl. Surf. Sci.*, 483 (2019) 901-911.
42. S. Abd El Wanees, A. Abd El Aal Mohamed, M. Abd El Azeem, R. El Said, Inhibition of silver corrosion in nitric acid by some aliphatic amines, *J. Disper. Sci. Technol.*, 31(2010)1516–1525.
43. T. K. Chaitra, K. N. Shetty Mohana, H. C.Tandon, Thermodynamic, electrochemical and quantum chemical evaluation of some triazole Schiff bases as mild steel corrosion inhibitors in acid media, *J. Mol. Liq.*, 211 (2015) 1026–1038.
44. N. Labjar, M. Lebrini, F. Bentiss, N. Chihib, S. El Hajjaji, C. Jama, Corrosion inhibition of carbon steel and antibacterial properties of aminotris-(methylenephosphonic) acid, *Mat. Chem. Phys.*, 119 (2010) 330–336.
45. A. Doner, R. Solmaz, M. Ozcan, G. Kardas, Experimental and theoretical studies of thiazoles as corrosion inhibitors for mild steel in sulphuric acid solution, *Corros. Sci.*, 53 (2011) 2902–2913
46. X.H. Li, S.D. Deng, H. Fu, G.N. Mu, Inhibition effect of 6-benzyl- amino purine on the corrosion of cold rolled steel in H<sub>2</sub>SO<sub>4</sub> solution, *Corros. Sci.*, 51 (2009) 620–634.
47. E.A. Noor, A.H. Al-Moubaraki, Thermodynamic study of metal corrosion and inhibitor adsorption processes in mild steel/1-methyl-4[4 (-X)-styryl pyridinium iodides/hydrochloric acid systems, *Mater. Chem. Phys.* 110 (2008) 145.
48. M. A. Hegazy, H. M. Ahmed, A. S. El-Tabei, Investigation of the inhibitive effect of p-substituted 4-(N,N,N-dimethyldodecylammonium bromide)benzylidene-benzene-2-yl-amine on

- corrosion of carbon steel pipelines in acidic medium, *Corros. Sci.*, 53 (2011) 671–6780.
49. M. A. Hegazy, Novel cationic surfactant based on triazole as a corrosion inhibitor for carbon steel in phosphoric acid produced by dihydrate wet process, *J. Mol. Liq.*, 208 (2015) 227-236.
50. M. F. El-Hady, H. A. H. Shehata, M. A. Hegazy, H. H. H. Hefni, Preparation of Some Eco-friendly Corrosion inhibitors having antibacterial activity from sea food waste, M. H. M. Hussein, *J. Surfact. Deterg.*, 16 (2013) 233–242.
51. E.E. Oguzie, Evaluation of the inhibitive effect of some plant extracts on the acid corrosion of mild steel, *Corros. Sci.*, 50 (2008) 2993–2998.
52. S. Abd El Wanees, Mohamed I. Alahmdi, M. Abd El Azzem, Hamdy E. Ahmed, 4,6-Dimethyl-2-oxo-1,2-dihydro-pyridine-3-carboxylic acid as an inhibitor towards the corrosion of C-steel in acetic acid, *Int. J. Electrochem. Sci.*, 11 (2016) 3448 - 3466.
53. S. A. Umoren, M. M. Solomon, U. M. Eduok, I. B. Obot, A. U. Israel, Inhibition of mild steel corrosion in H<sub>2</sub>SO<sub>4</sub> solution by coconut coir dust extract obtained from different solvent systems and synergistic effect of iodide ions: Ethanol and acetone extracts, *J. environ. Chem. eng.*, 2 (2014) 1048-1060.
54. C. Verma, E. E. Ebenso, Y. Vishal, M.A.Quraishi, Dendrimers: A new class of corrosion inhibitors for mild steel in 1 M HCl: Experimental and quantum chemical studies, *J. Mol. Liq.*, 224 (2016) 1282-1293.